Dielectric response of a semi-infinite HgTe/CdTe superlattice from its bulk and surface plasmons

Danhong Huang, Zhitang Lin
Department of Physics, Fudan University, Shanghai, People's Republic of China

Shixun Zhou
Department of Physics, Fudan University, Shanghai, People's Republic of China
(Received 6 September 1988; revised manuscript received 16 December 1988)

An analytic expression for the Raman-scattering cross section from both bulk and surface collective excitations in a semi-infinite HgTe/CdTe superlattice is derived. Calculations show that there exist three new branches for both intrasubband and intersubband surface plasmons. The optical surface plasmons possess a gap between bulk and surface modes. This dramatic feature will make the observation of existence of the surface plasmon in experiment feasible. The gap is explained in terms of additional energy exchange between surface modes and interface states.

I. INTRODUCTION

With recent advances in molecular-beam-epitaxy (MBE) technology, HgTe/CdTe superlattices can now be grown.[1,2] Collective charge-density excitations in HgTe/CdTe superlattices as well as in other superlattices recently received considerable attention.[3–6] The density-density correlation functions for the bulk, semi-infinite, and finite superlattices have been calculated.[7–9] The theory of resonant Raman scattering,[7–9] and electron-energy loss[9,10] (EEL) has been formulated. Bulk plasmons have been observed experimentally[11–13] in light scattering experiments. Surface plasmons still await detection, because it is difficult to satisfy the conditions that wave vector q should be greater than a critical one, q^*, in experiment. In addition, owing to the limited resolution of Raman spectrum, we have not yet detected the surface-plasmon modes in superlattices even in the case of a null critical wave vector.[14]

A HgTe/CdTe superlattice is a material which consists of both semimetal and wide-band-gap semiconductors. The Γ_6-Γ_8 energy bands in HgTe layers are reversed, as shown in Fig. 1, in contrast with those in CdTe layers to give the zero band gap. The computations of the band structure of HgTe/CdTe superlattices given by PWM,[15] linear combination of atomic orbitals[16,17] (LCAO) and envelope-function-approximation[18,19] (EFA) methods agree well and show that the electronlike, heavy-hole-like, and light-hole-like states are, as expected, confined very well in HgTe and CdTe layers.[1,2,17] On the other hand, Γ_8 energy bands in both HgTe and CdTe layers possess the effective masses with opposite signs on each side of the interface, respectively, which directly leads to the formation of a quasi-interface state with its energy lying between $0 < E_i < \Lambda$, where $\Lambda = V_p$ is the separation of Γ_8 energy bands in both HgTe and CdTe layers. Clearly, the electrons in HgTe layers will be in the quasi-interface states localized near the interface with the energy $E_i < \Lambda$. Moreover, light holes in CdTe layers will also be in the anomalous quasi-interface states localized near the interface, owing to the minus effective mass of the light hole. All of these results are consequences of matching the bulk states belonging to the conduction band in HgTe

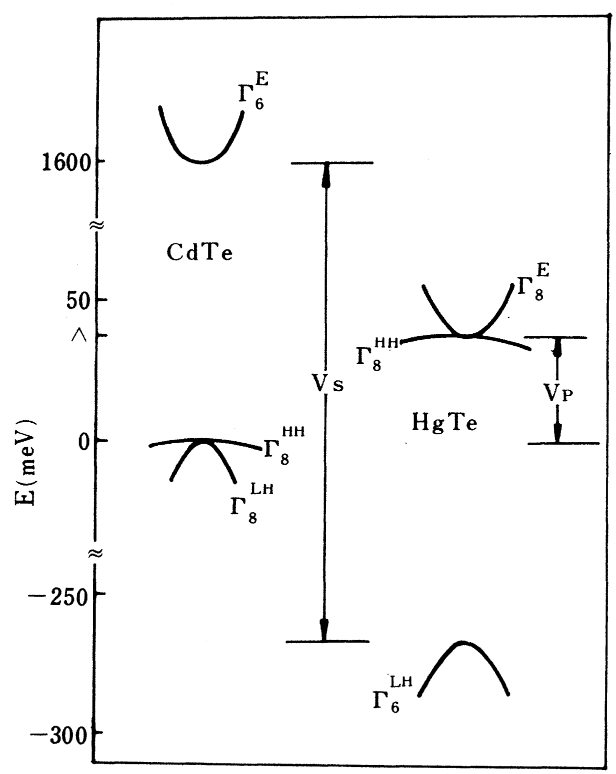

FIG. 1. Band structure of bulk HgTe and CdTe. The LH, HH, and E indices refer to light holes, heavy holes, and electrons, respectively.

with those belonging to the light-hole valence band in CdTe. This match is only favorable when the bulk states to be connected are made of atomic orbitals of the same symmetry type and the effective masses on either side of the interface have opposite signs. As a collective excitation model, we can treat the interface states in HgTe and CdTe layers as two different kinds of quasiparticles with the effective masses M_E and M_{LH} separately, just as the model given by Sham *et al.*[16,18]

It has been proven that the thickness of the materials, HgTe and CdTe, will mainly decide the width of the band gap and subbands, respectively. We assume the layers of HgTe and CdTe have the same thickness $d/2$ and d is smaller than the critical thickness $d_c=(2m_{\mathrm{LH}}/m_E^2\Lambda)^{1/2}$ so that a superlattice will behave like a semiconductor. It appears that the interface states play more important roles in HgTe-CdTe superlattices, in comparison with the situations in type-I and -II superlattices. Besides, we consider the motion of quasiparticles in the layers to be completely free. If d is not too small, we can neglect the tunneling effects coming from the overlap of interface states localized at adjacent interfaces in the quantum well. Indeed, when the planar wave vector $\mathbf{k}_\parallel$ is not very small, the hybridization between the interface states and the heavy-hole-like states will affect the fundamental gap of the material, which contributes a great deal to the transportation and the optical absorption.[14] We have partly taken this effect into consideration by using the wave functions with finite width of localization at interfaces, and including the coupling between the interface states and heavy-hole-like states. If we confine the study of collective excitation to the case in which the transitions of single particle are limited to the neighborhood of the Γ point of energy bands in the $\mathbf{k}$ space, we can neglect the hybridization in the band structure.[14] However, this hybridization can be taken into account by using a two-band tight-binding model. The study of coupled intrasubband and intersubband collective excitation modes of interface and heavy-hole-like states will be given in the Appendix. It proves that the simplification, which neglects the hybridization in the energy dispersion, is reasonable under certain conditions.

The goal of this paper is to give the calculation of collective excitations in HgTe/CdTe superlattices, including the surfaces modes, where a rich spectrum is expected. The paper is organized as follows: In Sec. II the model system is presented, and in Sec. III the density-density correlation function for this system is calculated, where three new bands for both intrasubband and intersubband surface plasmons have been found. They possess a dramatic gap between surface and bulk modes even for $q\to 0$, which is attributed to the additional surface Coulomb interaction at adjacent interfaces in the quantum well, induced by the breaking of translational symmetry in the superlattice direction.

This attractive feature will directly lead to the possibility of the detection of surface modes in experiment. The theories of Raman scattering and inelastic scattering are given in Sec. IV. It presents no fundamental difficulty in a numerical computation, although it has not been given here. Concluding remarks are contained in Sec. V.

II. THE MODEL SYSTEM

We now proceed to discuss the linear response of HgTe/CdTe superlattices to an external potential in the absence of a magnetic field. In our approximation given in the Introduction, the single-particle wave function in this model superlattice can be written as

$$|\mathbf{k},n,j\rangle=\exp(i\mathbf{k}\cdot\mathbf{r})\xi_n(z-jd/2)\ . \qquad (1)$$

Here $\mathbf{k}$ is a two-dimensional (2D) wave vector describing the planar motion in the (x,y) plane; j and n are the layer index and the subband index, respectively. We shall restrict our consideration only to the case of interface states. The layers are labeled by an integer j, even-numbered layers will be taken to be HgTe layers, in which electrons are confined, while odd-numbered layers are CdTe layers, in which light holes are confined. The noninteracting single-particle energy is given by

$$E_{nj}(\mathbf{k})=E_{nj}+\hbar^2k^2/2m_j\ . \qquad (2)$$

The system consists of a semi-infinite array of quantum wells, which are embedded in a medium, occupying the half-space $z>-d/4$, with a frequency-dependent dielectric function

$$\epsilon_s(\omega)=\epsilon_\infty(\omega^2-\omega_{\mathrm{L}}^2)/(\omega^2-\omega_{\mathrm{T}}^2)\ , \qquad (3)$$

where we have taken into account the electron-phonon coupling by replacing the background dielectric constant ϵ_S with $\epsilon_S(\omega)$ in Eq. (3).[8] ω_{L} and ω_{T} are the longitudinal- and transverse-optical–phonon frequencies. The other half-space is filled by an insulator with a dielectric constant ϵ_0. In this paper, we assume that only the lowest subband is filled at $T=0$, and the exchange-correlation potential V^{xc} is taken to be zero for convenience.

III. DENSITY-DENSITY CORRELATION FUNCTION

The density-density correlation function is the central quantity for calculations of Raman intensities and electron-energy-loss spectra. Following Ref. 9 we expand the density-density correlation function in the single-particle states

$$\Pi(q,\omega;z,z')=\sum_{i,j;p,t}\ \sum_{l,l';l'',l'''}\Pi_{i,j;p,t}(l,l',l'',l''')\xi_i(z-ld/2)\xi_j(z-l'd/2)\xi_p(z'-l''d/2)\xi_t(z'-l'''d/2)\ . \qquad (4)$$

In the random-phase approximation (RPA), $\Pi_{i,j;p,t}(l,l';l'',l''')$ satisfies the Dyson integral equation

$$\Pi_{i,j;p,t}(l,l';l'',l''')=\Pi^0_{i,j}(l,l)\delta_{it}\delta_{jp}\delta_{ll'}\delta_{l'l''}\delta_{l''l'''}+\sum_{r,s}\ \sum_{m,m'}\Pi^0_{i,j}(l,l)V_{i,j;r,s}(l,l';m,m')\Pi_{r,s;p,t}(m,m';l'',l''')\ , \qquad (5)$$

where $\Pi^0_{i,j}(l,l)$ is the polarizability of the noninteracting system, and $V_{i,j;r,s}(l,l',m,m')$ is the Coulomb interaction, including the effect of image charges and subband structure. Furthermore, we employ the commonly used diagonal approximation,[20] which decouples different intersubband excitations. Then Eq. (5) can be rewritten as

$$\Pi_{i,j}(l,l';l'',l''')=\Pi^0_{i,j}(l,l)\delta_{ll'}\delta_{l'l''}\delta_{l''l'''}+\sum_{m,m'}\Pi^0_{i,j}(l,l)V_{i,j;i,j}(l,l',m,m')\Pi_{i,j}(m,m';l'',l''') . \tag{6}$$

Under the electric quantum limit, Eq. (6) gives

$$\chi_n(l,l';l'',l''')=\chi^0_n(l,l)\delta_{ll'}\delta_{l'l''}\delta_{l''l'''}+\sum_{m,m'}\chi^0_n(l,l)V_{n,n}(l,l';m,m')\chi_n(m,m';l'',l''') , \tag{7}$$

where $\chi^0_n=\Pi^0_{0,n}+\Pi^0_{n,0}$ for $n\neq 0$ and $\chi^0_0=\Pi^0_{0,0}$. The substitution of Eq. (7) reduces Eq. (4) to the form

$$\chi(q,\omega;z,z')=\sum_n\sum_{l,l';l'',l'''}\chi_n(l,l';l'',l''')\times\Psi_n(l,l';z)\Psi_n(l'',l''',z') \tag{8}$$

with the symbols given by

$$\Psi_n(l,l';z)=\xi_n(z-ld/2)\xi_0(z-l'd/2) . \tag{9}$$

A lengthy manipulation will further lead Eq. (8) to

$$\chi(q,\omega;z,z')=\sum_n\sum_{l,l'}\chi_n(l,l')\times\Phi_n(z-ld/2)\Phi_n(z'-l'd/2) \tag{10}$$

with

$$\Phi_n(z-jd/2)=\Psi_n(j,j;z)+[\Psi_n(j+1,j;z)+\Psi_n(j-1,j;z)+\Psi_n(j,j+1;z)+\Psi_n(j,j-1;z)]/2 . \tag{11}$$

Following Refs. 8 and 9, we now Fourier transform all quantities, e.g.,

$$\underline{\chi}_n(k,k')=(1/N)\sum_{j,j'}\exp(-ikjd/2)\underline{\chi}_n(j,j')\exp(ik'j'd/2)=\begin{bmatrix}\chi^{e\text{-}e}_n(k,k') & \chi^{e\text{-}h}_n(k,k')\\ \chi^{h\text{-}e}_n(k,k') & \chi^{h\text{-}h}_n(k,k')\end{bmatrix} , \tag{12}$$

where $k=2n\pi/Nd$, $n=0,1,2,\ldots,N-1$, d is the period of the superlattice, and even and odd "j" refer to electronlike and light-hole-like states, respectively. The Fourier transform of Eq. (10) gives

$$\underline{\chi}_n(k,k')=\underline{\chi}_0\delta_{kk'}+v_q\sum_{k''}\underline{\chi}_0\underline{f}_{nn}(k,k'')\underline{\chi}_n(k'',k') , \tag{13}$$

where $v_q=2\pi e^2/\epsilon_s(\omega)q$, and

$$\underline{\chi}_0=\begin{bmatrix}\chi^e_n & 0\\ 0 & \chi^h_n\end{bmatrix} .$$

Here $\underline{f}_{nn}(k,k')$ is the Fourier transform of the Coulomb interaction $\underline{V}_{nn}(l,l')$. We write $\underline{\chi}_n(k,k')$ and $\underline{f}_{nn}(k,k')$ in terms of the "bulk" and "surface" parts where bulk part merely means a part diagonal in **k** space and surface part is the rest:

$$\underline{\chi}_n(k,k')=\underline{\chi}^B_n(k)\delta_{kk'}+\underline{\chi}^s_n(k,k') , \tag{14}$$

$$\underline{f}_{nn}(k,k')=\underline{f}^B_n(k)\delta_{kk'}+\underline{f}^s_n(k,k') . \tag{15}$$

The explicit forms of $\underline{\chi}^B_n(k)$ and $\underline{f}^B_n(k)$ can be given by

$$\underline{\chi}^B_n(k)=[\underline{I}-\underline{\chi}_0v_q\underline{f}^B_n(k)]^{-1}\underline{\chi}_0 , \tag{16}$$

$$\underline{f}^B_n(k)=\{\underline{r}_{-n}(q)[\exp(-ikd)-\exp(-qd)]+\underline{r}_{-n}(-q)[\exp(ikd)-\exp(-qd)]\}/2P(k)+\underline{V}_{-n}(q) , \tag{17}$$

with

$$\underline{r}_{\pm n}(q)=\begin{bmatrix}G_{\pm n}(q) & \exp(\mp qd/2)G_{\pm n}(q)\\ \exp(-qd/2)G_{\pm n}(q) & G_{\pm n}(q)\end{bmatrix} , \tag{18}$$

$$\underline{V}_{-n}(q)=\begin{bmatrix}V_{-n}(q) & \exp(-qd/2)G_{-n}(q)\\ \exp(-qd/2)G_{-n}(q) & V_{-n}(q)\end{bmatrix} , \tag{19}$$

where the symbols $G_{\pm n}(q)$ and $V_{-n}(q)$ are given by

$$G_{\pm n}(q)=\tfrac{1}{2}\int_{-d/4}^{\infty}dz\int_{-d/4}^{\infty}dz'\,\Phi_n(z)\Phi_n(z')\times\exp[-q(z\pm z')] , \tag{20}$$

$$V_{-n}(q)=\tfrac{1}{2}\int dz'\Phi_n(z)\Phi_n(z')\exp(-q|z-z'|) , \tag{21}$$

and $P(k)=\cosh(qd)-\cos(kd)$. Furthermore, we straightforwardly write down the surface part of Coulomb interaction:

$$f^s_n(k,k')=\{[1-\exp(-qdN)]/4NP(k)P(k')\}\times\{\underline{a}-\underline{b}_1\exp(ikd)-\underline{b}_2\exp(-ik'd)+\underline{c}\exp[i(k-k')d]\} , \tag{22}$$

where

$$\underline{a}=[\underline{r}_{-n}(q)+\underline{r}_{-n}(-q)]+\alpha\underline{r}_{+n}(q)\exp(2qd) , \tag{23}$$

$$\underline{b}_1=[\underline{r}_{-n}(q)\exp(-qd)+\underline{r}_{-n}(-q)\exp(qd)]+\alpha\underline{r}_{+n}(q)\exp(qd) , \tag{24}$$

$$\underline{b}_2=[\underline{r}_{-n}(q)\exp(qd)+\underline{r}_{-n}(-q)\exp(-qd)]+\alpha\underline{r}_{+n}(q)\exp(qd)\ , \tag{25}$$

$$\underline{c}=[\underline{r}_{-n}(q)+\underline{r}_{-n}(-q)]+\alpha\underline{r}_{+n}(q)\ , \tag{26}$$

$$\alpha=[1-\exp(-qdN)]\exp(-qd/2)\times[\epsilon_s(\omega)-\epsilon_0]/[\epsilon_s(\omega)+\epsilon_0]\ . \tag{27}$$

By using the *ansatz* for $\underline{\chi}_n^s(k,k')$ (Ref. 9) in Eqs. (13)–(15), we get

$$\underline{\chi}_n^s(k,k')=\{[1-\exp(-qdN)]/4NP(k)P(k')\}\underline{\chi}_n^B(k)\times\{\underline{A}-\underline{B}_1\exp(ikd)-\underline{B}_2\exp(-ik'd)+\underline{C}\exp[i(k-k')d]\}\underline{\chi}_n^B(k') \tag{28}$$

with the coefficients given by the following equations:

$$\begin{bmatrix}\underline{A}\\ \underline{B}_1\end{bmatrix}=\underline{M}^{-1}\begin{bmatrix}\underline{a}\\ \underline{b}_1\end{bmatrix}\quad\text{and}\quad\begin{bmatrix}\underline{B}_2\\ \underline{C}\end{bmatrix}=\underline{M}^{-1}\begin{bmatrix}\underline{b}_2\\ \underline{c}\end{bmatrix}\ , \tag{29}$$

where

$$\underline{M}=\begin{bmatrix}\underline{I}-\underline{a}\,\underline{G}-\underline{b}_2\underline{H}_- & \underline{a}\,\underline{H}_+-\underline{b}_2\underline{G}\\ \underline{c}\,\underline{H}_--\underline{b}_1\underline{G} & \underline{I}-\underline{c}\,\underline{G}+\underline{b}_1\underline{H}_-\end{bmatrix}\ , \tag{30}$$

$$\underline{G}=\{v_q[1-\exp(-qdN)]/4N\}\sum_k\underline{\chi}_n^B(k)/P(k)^2\ , \tag{31}$$

$$\underline{H}_\pm=\{v_q[1-\exp(-qdN)]/4N\}\times\sum_k\exp(\pm ikd)\underline{\chi}_n^B(k)/P(k)^2\ . \tag{32}$$

Poles of the density-density correlation function $\chi_n(k,k')$ define collective excitations of the superlattice. When the number of layers N is very large ($N\rightarrow\infty$), bulk plasmons are given by the poles of the bulk part while surface plasmons are given by the poles of the surface part. For a finite number of layers, the full solution must be used. The finite-size effect will give $2N$ discrete collective modes[9] if we ignore the electron-phonon coupling. Here we are only interested in the semi-infinite superlattice system ($N\rightarrow\infty$); thus we can get bulk and surface plasmons from Eqs. (16) and (28), respectively.

First, we shall neglect the electron-phonon coupling. Then for intrasubband excitation, we have

$$\xi_0(z)=\begin{cases}D\exp(\beta d/4)[\exp(\beta z)+\exp(-\beta d)\exp(-\beta z)], & -3d/4\le z\le -d/4 \quad (33a)\\ D\exp(-\beta d/4)[\exp(\beta z)+\exp(-\beta z)], & -d/4\le z\le d/4 \quad (33b)\\ D\exp(\beta d/4)[\exp(-\beta z)+\exp(-\beta d)\exp(\beta z)], & d/4\le z\le 3d/4 \quad (33c)\end{cases}$$

with the normalization factor

$$D=\exp(\beta d/4)/[d+2\sinh(\beta d/2)/\beta]^{1/2} \tag{34}$$

and the long-wavelength form of $\chi_0^{e,h}(\mathbf{q},\omega)$

$$\chi_0^{e,h}(\mathbf{q},\omega)=n_{e,h}q^2/m_{e,h}\omega^2\ . \tag{35}$$

The ratio of the plasma frequencies for the electron and hole layers is $\gamma=[\omega_{pe}(q)]^2/[\omega_{ph}(q)]^2$. Then we get the analytic solution

$$\omega_\pm^2=\{[\omega_{pe}(q)]^2+[\omega_{ph}(q)]^2]\}[V_-+(S-1)G_-]/2+\{[\omega_{pe}(q)]^2-[\omega_{ph}(q)]^2\}^2[V_-+(S-1)G_-]^2+4[\omega_{pe}(q)]^2[\omega_{ph}(q)]^2(S')^2G_-^2\}^{1/2}/2\ , \tag{36}$$

where

$$G_-=\{4[2+\exp(-\beta d/2)]/[d+2\sinh(\beta d/2)/\beta]^2\}\times[\sinh[(2\beta+q)d/4]/(2\beta+q)+\sinh[(2\beta-q)d/4]/(2\beta-q)+2\sinh(qd/4)q]^2\ , \tag{37}$$

$$\begin{aligned}V_-=\{4[2+\exp(-\beta d/2)]/[d+2\sinh(\beta d/2)/\beta]^2\}&\\ \times(2q/(q^2-4\beta^2)[\sinh(\beta d/2)/\beta+\sinh(\beta d)/4\beta+d/4]+[d+2\sinh(\beta d/2)/\beta]/q&\\ -\{\exp[-(2\beta+q)d/4]/(2\beta+q)-\exp[(2\beta-q)d/4]/(2\beta-q)+2\exp(-qd/4)/q\}&\\ \times\{\sinh[(2\beta+q)d/4]/(2\beta+q)+\sinh[(2\beta-q)d/4]/(2\beta-q)+2\sinh(qd/4)/q\})\ ,&\end{aligned} \tag{38}$$

which is just the result presented in Ref. 3. Here we have introduced the structure factors S and S' defined by

$$S(\mathbf{q},k)=\sinh(qd)/P(k)\ , \tag{39}$$

$$S'(\mathbf{q},k)=2\cos(kd/2)\sinh(qd/2)/P(k)\ . \tag{40}$$

On the other hand, for intersubband excitation, we have

$$\xi_1(z)=\begin{cases} C\exp(-\beta d/4)\{\exp[-\beta(z+d/2)]-\exp[\beta(z+d/2)]\}, & -3d/4\le z\le -d/4 \quad (41a)\\ C\exp(-\beta d/4)[\exp(\beta z)-\exp(-\beta z)], & -d/4\le z\le d/4 \quad (41b)\\ C\exp(-\beta d/4)\{\exp[-\beta(z-d/2)]-\exp[\beta(z-d/2)]\}, & d/4\le z\le 3d/4 \quad (41c)\end{cases}$$

with the normalization factor

$$C=\exp(\beta d/4)/[2\sinh(\beta d/2)/\beta-d]^{1/2} \tag{42}$$

and the long-wavelength form of $\chi_1^{e,h}(\mathbf{q},\omega)$ to the order of q,

$$\chi_1^{e,h}(\mathbf{q},\omega)=2n_{e,h}\Omega_{10}/\hbar(\omega^2-\Omega_{10}^2) \; . \tag{43}$$

This leads to the following analytic result:

$$\omega_\pm^2=\Omega_{10}^2\{1+(\alpha_e+\alpha_h)[V_{-n}+(S-1)G_{-n}]/qd\}\pm(\Omega_{10}^2/qd)\{(\alpha_e-\alpha_h)^2[V_{-n}+(S-1)G_{-n}]^2+4\alpha_e\alpha_h(S')^2G_{-n}^2\}^{1/2} \; , \tag{44}$$

where

$$\alpha_{e,h}=[(2n_{e,h}/\hbar\Omega_{10})(2\pi e^2/\epsilon_s)](d/2) \; , \tag{45}$$

the ratio of parameters $\alpha_{e,h}$ is $\gamma'=\alpha_e/\alpha_h$, and

$$G_{-n}=\{-8/[4\sinh^2(\beta d/2)/\beta^2-d^2]\}\{\sinh[(2\beta-q)d/4]/(2\beta-q)-\sinh[(2\beta+q)d/4]/(2\beta+q)\}^2 \; , \tag{46}$$

$$\begin{aligned} V_{-n}=&\{8/[4\sinh^2(\beta d/2)/\beta^2-d^2]\}\\ &\times(q[\sinh(\beta d)-\beta d]/2\beta(q^2-4\beta^2)+\{\exp[-(2\beta+q)d/4]/(2\beta+q)+\exp[(2\beta-q)d/4](2\beta-q)\}\\ &\quad\times\{\sinh[(2\beta+q)d/4]/(2\beta+q)-\sinh[(2\beta-q)d/4]/(2\beta-q)\}) \; , \end{aligned} \tag{47}$$

which has been predicted in Ref. 4.

The surface plasmons for both intrasubband and intersubband excitations can be determined by zeros of the determinant of matrix $\underline{M}$, and $\underline{M}$ is given by Eq. (30).

All the results, taking the electron-phonon coupling into consideration, are presented in Figs. 2–5 for both intrasubband and intersubband excitations.

From Figs. 2 and 3, we can see that there exist four bulk modes $I_1^0-I_4^0$, two of which come from the splitting, owing to the electron-phonon coupling. The interaction between optical phonons and bulk plasmons is responsible for the optical-phonon bands I_2^0 and I_3^0. I_1^0 and I_4^0 are the optical and acoustical bulk plasmon, respectively. Moreover, there are two optical-phonon–surface-plasmon modes S_2^0 and S_3^0, one optical surface-plasmon mode S_1^0, and one acoustical surface-plasmon mode S_4^0. O_1^0 mode is a new optical-phonon–surface-plasmon mode S_1^0, and one acoustical surface-plasmon mode S_4^0. The O_1^0 mode is a new optical-phonon–surface-plasmon mode in the intrasubband excitations, which, to our knowledge, has never been reported before. It should be noted that the existence of a gap between S_1^0 and I_1^0 modes can be explained as the additional surface Coulomb interaction between neighboring interfaces.

From Figs. 4 and 5, we know that there are four bulk modes $I_1^1-I_4^1$. Among them I_3^1 and I_4^1 are two optical-phonon bands, coming from the electron-phonon coupling. There are also two optical-phonon–surface-plasmon modes $S_3^1-S_4^1$ as well as the other two surface hodes $S_1^1-S_2^1$ associated with intersubband excitations. Note, however, that there are two extra modes O_1^1 and O_2^1 with frequencies below ω_L associated with the 0-1 intersubband transition, in which the O_1^1 mode has been predicted by Quinn *et al.*,[8] while the O_2^1 mode is a new one not reported previously. The dramatic feature is that there also exists a gap between S_2^1 and I_2^1 modes. The reason for the existence of this gap is analogous to that in the intrasubband excitation. We can easily see that both I_1^1 and I_4^1 modes are reversed in Figs. 4 and 5. A superlattice analog of the trapped surface modes in accumulation layers has been recently discovered by Puri and Schaich.[21]

IV. RAMAN INTENSITIES

We now turn to Raman intensity, which is proportional[8,9,22] to the function $F(\omega,Q)$ in Eq. (48),

$$F(\omega,\mathbf{Q})=-\sum_n A_n\mathrm{Im}[\chi_n^{e\text{-}e}(2k_z^*,2k_z)+\chi_n^{e\text{-}h}(2k_z^*,2k_z)+\chi_n^{h\text{-}e}(2k_z^*,2k_z)+\chi_n^{h\text{-}h}(2k_z^*,2k_z)] \; , \tag{48}$$

where

$$\omega=\omega_i-\omega_s$$

and

$$\mathbf{Q}=(\mathbf{q},k_z)=(\mathbf{q}_i-\mathbf{q}_s,k_z^i+k_z^s) \; .$$

We now make the approximation[8,9]

$$k_z^i = k_z^s = k + i/2\lambda \ ,$$

where

$$k = (\omega_i / c)\mathrm{Re}[\epsilon_s(\omega_i)]^{1/2}$$

and

$$1/\lambda = (2\omega_i / c)\mathrm{Im}[\epsilon_s(\omega_i)]^{1/2} \ .$$

$2k$ is thus the momentum transfer to the plasmon from a photon along the superlattice axis, and λ is the photon decay length inside the material. A_n is an amplitude given by

$$A_n = \exp(-d/2\lambda)\int dz \int dz' \exp[-2ik(z-z')] \times \exp[-(z+z')/\lambda] \times \Phi_n(z)\Phi_n(z') \ . \quad (49)$$

The terms $n=0$ and $n=1$ stand for the contributions from intrasubband and intersubband excitations, respectively. Here the density-density correlation function $\underline{\chi}_n(k,k')$ and $\Phi_n(z)$ are given by Eqs. (16), (28), and (11).

It should be noted that the single-particle energy separation Ω_{10} of interface states is identical for both electrons and light holes, so that we must take into account all the terms of $\underline{\chi}_n(k,k')$ in Eq. (48). This means that the light will couple to electrons, as well as light holes in interface states. Instead of Eqs. (3), (35), and (43), we use

$$\epsilon_s(\omega) = \epsilon_\infty(\omega^2 - \omega_{\mathrm{LO}}^2 + i\gamma_{\mathrm{ph}}\omega)/(\omega^2 - \omega_{\mathrm{TO}}^2 + i\gamma_{\mathrm{ph}}\omega) \quad (50)$$

γ_{ph} being the phenomenological width, and

$$\chi_0^{e,h} = n_{e,h} q^2 / m_{e,h}(\omega^2 + i\gamma_{e,h}\omega) \ , \quad (51)$$

$$\chi_1^{e,h} = 2n_{e,h}\Omega_{10}/\hbar(\omega^2 - \Omega_{10}^2 + i\gamma_{e,h}\omega) \ , \quad (52)$$

$\gamma_{e,h}$ being the phenomenological broadening, related to mobility in the usual way. The peaks in the spectrum correspond to the poles of the polarizability matrix $\underline{\chi}_n(k,k')$. The broadening of the bulk and surface plasmons is due to phonon decay and the parameters $\gamma_{e,h}$ separately.[8]

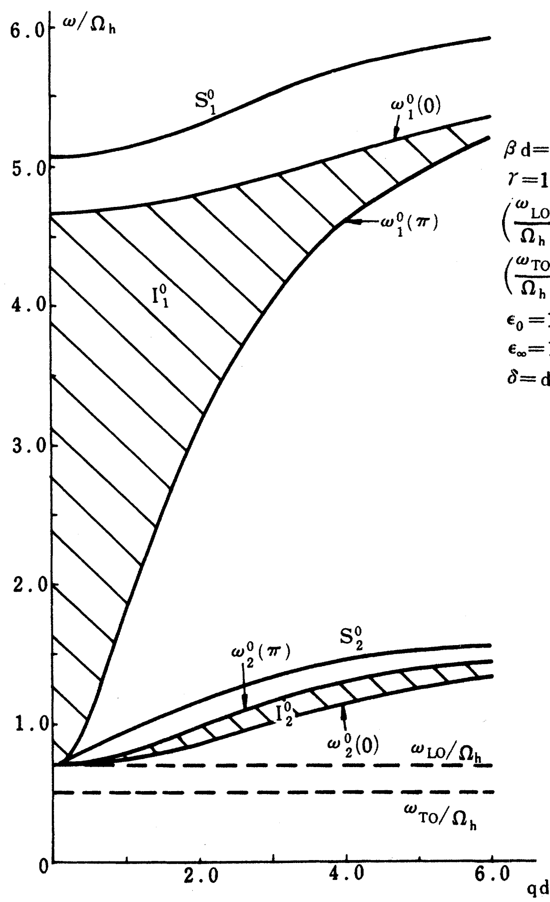

FIG. 2. Two higher branches of the collective intrasubband excitation spectrum for phonon-plasmon modes in quasi-2D interfaces with the parameters $\beta d = 0.7742$, $\epsilon_\infty = 16.0$, $\epsilon_0 = 1.0$, $\gamma = 15.0$, $(\omega_{\mathrm{L}}/\Omega_h)^2 = 0.5$, and $(\omega_{\mathrm{T}}/\Omega_h)^2 = 0.25$.

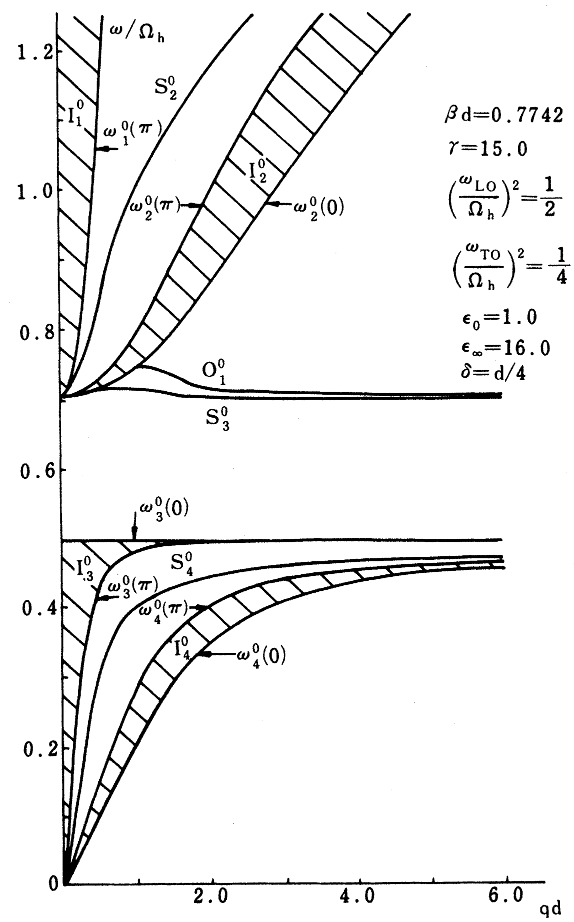

FIG. 3. Two lower branches of the collective intrasubband excitation spectrum for phonon-plasmon modes in quasi-2D interfaces. The parameters are the same as in Fig. 2.

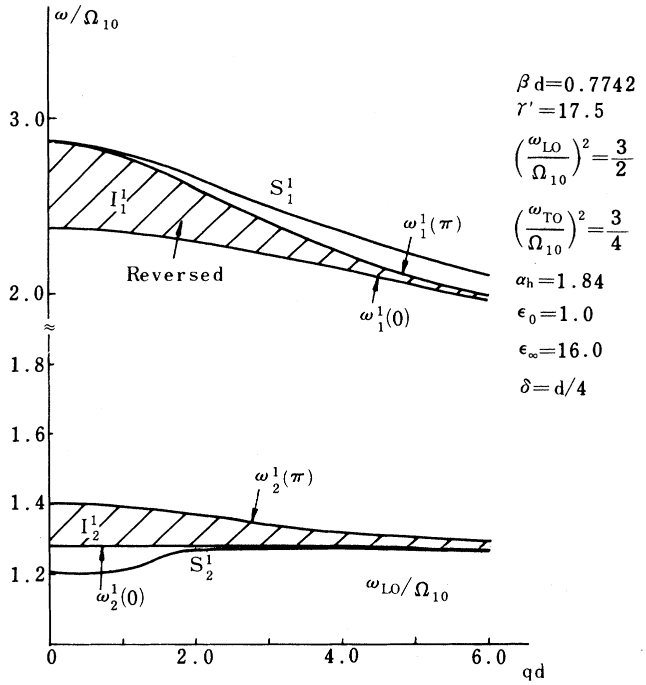

FIG. 4. Two higher branches of the collective intersubband excitation spectrum for phonon-plasmon modes in quasi-2D interfaces with the parameters $\beta d = 0.7742$, $\epsilon_\infty = 16.0$, $\epsilon_0 = 1.0$, $\gamma' = 17.5$, $(\omega_L/\Omega_{10})^2 = \frac{3}{2}$, and $(\omega_T/\Omega_{10})^2 = \frac{3}{4}$, and $\alpha_h = 1.84$.

V. CONCLUDING REMARKS

In summary, we have presented the theory of collective excitation, including the bulk and surface modes, in a semi-infinite HgTe/CdTe superlattice. The density-density correlation function has been calculated and several new plasmon modes have been predicted. The theory can be easily extended to the finite-size superlattice. Moreover, we have formulated the theory of Raman scattering. In Raman-scattering experiments the intensity of the intersubband modes is higher than that of the intrasubband modes,[8] but the gap between S_2^1 and I_2^1 modes is smaller than that between S_1^0 and I_1^0 modes. The intersubband surface modes may be easily observed in experiment. This will make it easy to detect the existence of the surface-plasmon mode when a large gap exists between S_1^0 and I_1^0 modes, or S_2^1 and I_2^1 modes.[23,24]

ACKNOWLEDGMENTS

This work was supported by the Chinese Natural Science Foundation through Grant No. 18760723.

APPENDIX

In this appendix we would like to calculate the hybridization between the interface states and heavy-hole-like states and show that this effect will not make much change in the spectra of interface states given in Figs. 2–5.

Introducing the index $\alpha = 1,2,3$ representing the light-hole-like, electronlike, and heavy-hole-like states, respectively, we have

$$|\mathbf{k},n,j;\alpha\rangle = \exp(i\mathbf{k}\cdot\mathbf{r})\xi_n^{(\alpha)}(z - jd/2) \; . \tag{A1}$$

Here k is a two-dimensional wave vector describing the planar motion in the (x,y) plane; j and n are the layer index and the subband index, respectively. The layers are labeled by an integer j; even-numbered layers will be taken to be HgTe layers, in which electrons and heavy holes are confined, while odd-numbered layers are CdTe layers, in which light holes are confined. The single-particle energy is given by

$$E_{nj}^{(\alpha)}(\mathbf{k}) = E_{nj}^{(\alpha)} + \hbar^2 k^2 / 2m_j^{(\alpha)} \; . \tag{A2}$$

Generally, $m_j^{(\alpha)}$ will depend on the planar wave vector $\mathbf{k}_\parallel$. If the single-particle transitions are limited to the neighborhood of the Γ point of energy bands in $\mathbf{k}$ space, the

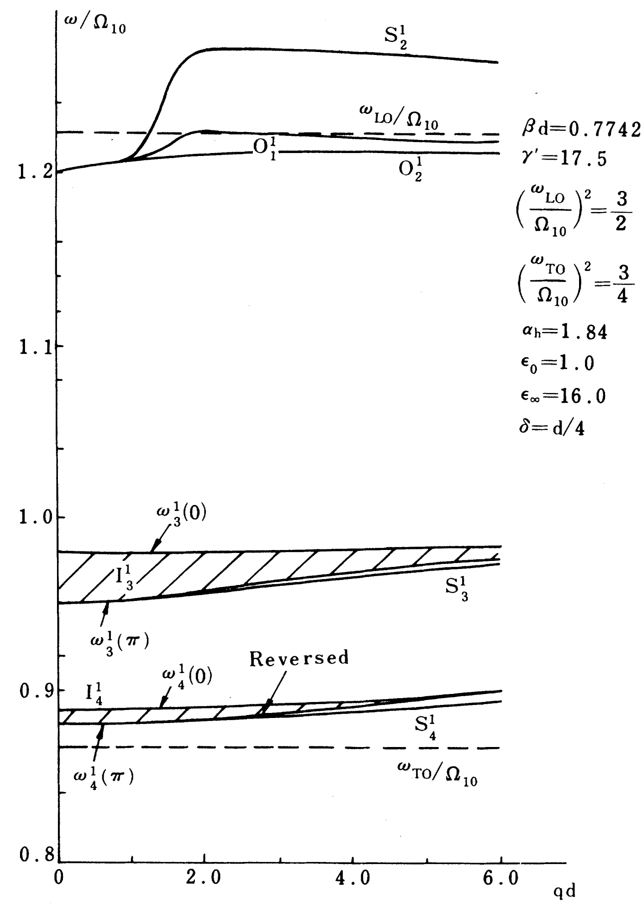

FIG. 5. Two lower branches of the collective intersubband excitation spectrum for phonon-plasmon modes in quasi-2D interfaces. The parameters are the same as in Fig. 4.

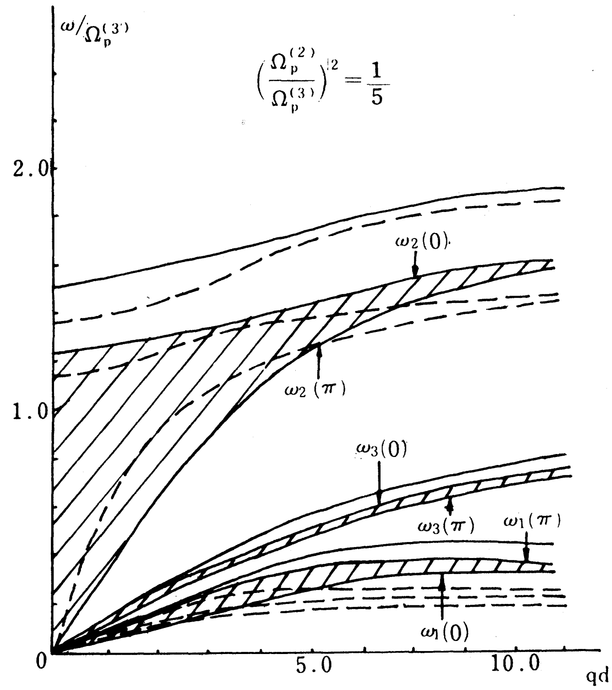

FIG. 6. The coupled collective intrasubband excitation spectra of interface and heavy-hole-like states with finite width of localization at the interfaces.

dominant term no longer depends on $\mathbf{k}_{\parallel}$ (the zeroth-order approximation), and then Eq. (2) is still applicable in this case.

It should be pointed out that it is really difficult to calculate the analytical expression of the energy dispersion for both interface states and heavy-hole-like states with hybridization. Fortunately, the effect of the nonparabolic energy dispersion relation cannot qualitatively change the feature of the collective excitation spectrum of interface states, although it contributes a great deal to the transportation and the optical absorption. The gap between the bulk optical plasmon mode and the surface mode will remain. Only the branch edges in the spectrum are quantitatively changed or shifted.

The effect of hybridization is reflected in three aspects, including the finite width of localization of interface states, the Coulomb interaction between the interface states and the heavy-hole-like states, and the nonparabolic energy dispersion relation.

Taking into account the first two aspects, we rewrite Eq. (10) as

$$\chi(q,\omega;z,z')=\sum_{\alpha,\alpha'}\sum_{n}\sum_{l,l'}\chi_n^{(\alpha,\alpha')}(l,l')\Phi_n^{(\alpha)}(z-ld/2)\times\Phi_n^{(\alpha')}(z'-l'd/2)\ , \tag{A3}$$

where $\Phi_n^{(1,2)}(z-jd/2)$ have the same definition as in Eq. (11), and

$$\Phi_n^{(3)}(z-jd/2)=\xi_n^{(3)}(z-jd/2)\xi_0^{(3)}(z-jd/2)\ . \tag{A4}$$

We would like to give the expressions below which have different definitions than before, and omit those with the same definitions. By using the substitutions of $\underline{\chi}_0$, $\underline{r}_{\pm n}$, and $\underline{V}_{-n}$ with Eqs. (A5)–(A8),

$$\underline{\chi}_0=\begin{bmatrix}\chi_n^h & 0 & 0\\ 0 & \chi_n^e & 0\\ 0 & 0 & \chi_n^{\mathrm{HH}}\end{bmatrix}\ , \tag{A5}$$

$$\underline{S}_{\pm n}(q)=\tfrac{1}{2}\exp[-q(d_\alpha\pm d'_\alpha)/2]\int dz\int dz'\,\Phi_n^{(\alpha)}(z)\Phi_n^{(\alpha')}(z')\exp[-q(z\pm z')]\ , \tag{A6}$$

$$\underline{t}_{-n}(q)=\tfrac{1}{2}\exp[-q|d_\alpha-d'_\alpha|/2]\int dz\int dz'\,\Phi_n^{(\alpha)}(z)\Phi_n^{(\alpha')}(z')\exp(-q|z-z'|)\ , \tag{A7}$$

$$d_\alpha=\begin{cases}d & \text{for light-hole-like states}\\ 0 & \text{for electronlike and heavy-hole-like states}\end{cases} \tag{A8}$$

into Eqs. (22) and (33), we can get both the bulk and the surface modes.

The computational result is presented in Fig. 6. The solid lines in Fig. 6 stand for the modes with hybridization, and the dashed lines for the modes without hybridization. The electron-phonon coupling has not been taken into account in Fig. 6 for simplicity. The optical plasmon mode of heavy branch ω_3 disappears here. It is clear that the qualitative feature of the collective excitation spectrum of interface states, e.g., the gap between the bulk and surface modes, is still retained, which, to a certain extent, proves that the conclusions drawn here are quite reasonable.

[1]J. M. Berroir, Y. Guldner, and M. Voos, IEEE J. Quantum Electron. **QE-22**, 1793 (1986).
[2]J.-P. Faurie, IEEE J. Quantum Electron. **QE-22**, 1656 (1986).
[3]Dan-hong Huang and Shi-xun Zhou, Phys. Rev. B **38**, 13 061 (1988).
[4]Dan-hong Huang and Shi-xun Zhou, **38**, 13 069 (1988).
[5]A. C. Tselis and J. J. Quinn, Phys. Rev. B **29**, 3318 (1984).
[6]G. F. Gilulian and J. J. Quinn, Phys. Rev. Lett. **51**, 919 (1983).

[7]Jainendra K. Jain and Philip B. Allen, Phys. Rev. B **32**, 997 (1985).
[8]Pawel Hawrylak, Ji-W. Wu, and J. J. Quinn, Phys. Rev. B **32**, 5169 (1985).
[9]Pawel Hawrylak, Gunnar Eliasson, and J. J. Quinn, Phys. Rev. B **34**, 5368 (1986).
[10]Pawel Hawrylak, Ji-W. Wu, and J. J. Quinn, Phys. Rev. B **32**, 4272 (1985).
[11]D. Olego, A. Pinczuk, A. C. Gossard, and W. Wiegmann, Phys. Rev. B **25**, 7867 (1982).
[12]R. Sooryakumar, A. Pinczuk, A. C. Gossard, and W. Wiegmann, Phys. Rev. B **31**, 2578 (1985).
[13]A. Pinczuk, M. G. Lamont, and A. C. Gossard, Phys. Rev. Lett. **56**, 2092 (1986).
[14]Y. Zhu, S. Cai, and Shi-xun Zhou, Phys. Rev. B **38**, 9941 (1988).
[15]D. Mukherji and B. R. Nag, Phys. Rev. B **12**, 4338 (1957).
[16]Y.-C. Chang, J. N. Schulman, G. Bastard, Y. Guldner, and M. Voos, Phys. Rev. B **31**, 2557 (1985).
[17]M Jaros, A. Zoryk, and D. Ninno, Phys. Rev. B **35**, 8277 (1987).
[18]Y. R. Lin-Liu and L. J. Sham, Phys. Rev. B **32**, 5561 (1985).
[19]G. Bastard, Phys. Rev. B **25**, 7584 (1982).
[20]G. H. Kawamoto, J. J. Quinn, and W. L. Bloss, Phys. Rev. B **23**, 1785 (1981); D. L. Dahl and L. J. Sham, *ibid.* **16**, 651 (1977).
[21]A. Puri and W. L. Schaich, Phys. Rev. B **31**, 974 (1985).
[22]J. K. Jain and P. B. Allen, Phys. Rev. Lett. **54**, 947 (1985).
[23]W. L. Shaich, Phys. Rev. B **24**, 686 (1981).
[24]R. E. Camley and D. L. Mills, Phys. Rev. B **29**, 1695 (1984).